# Dielectric-Spectroscopic and a.c. Conductivity Studies on Layered Na2-XKXTi3O7 (X=0.2, 0.3, 0.4) Ceramics

3 AUTHORS:

Deepam Maurya
Virginia Polytechnic Institute and State Uni...
**80** PUBLICATIONS   **457** CITATIONS

SEE PROFILE

Jitendra Kumar
Indian Agricultural Research Institute
**6** PUBLICATIONS   **73** CITATIONS

SEE PROFILE

Shripal Sharma
Pandit Prithi Nath College
**18** PUBLICATIONS   **87** CITATIONS

SEE PROFILE

ELSEVIER

# Dielectric-spectroscopic and a.c. conductivity studies on layered Na$_{2-X}$K$_X$Ti$_3$O$_7$ (X=0.2, 0.3, 0.4) ceramics

Deepam Maurya[a], Jitendra Kumar[b], Shripal[a],*

[a]Department of Physics, P.P.N. College Kanpur-208001, India
[b]Materials Science Programme, I.I.T. Kanpur-208016, India

## Abstract

The dependence of loss tangent (tanδ) and relative permittivity (ε$_r$) on temperature and frequency has been reported for Na$_{2-X}$K$_X$Ti$_3$O$_7$ (with X=0.2, 0.3, 0.4) ceramics. The losses are characteristic of dipole mechanism and electrical conduction. The peaks of ε$_r$ at high temperature indicate a possible ferroelectric phase transition for all three compositions. The results of a.c. conductivity studies on the same samples have also been reported. The corresponding ln(σT) versus 1000/T plots have been divided into five regions namely I, II, III, IV and V. The various conduction mechanisms in the different regions have been stressed. Furthermore, the log(σ) versus frequency plots for all the above samples reveal that the electronic hopping (polaron) conduction, which diminishes with the rise in temperature, is dominant in the lower temperature region. The interlayer ionic conduction seems to play a major role in conduction towards higher temperature.

## 1. Introduction

The crystal structure of layered Na$_2$Ti$_3$O$_7$ was first reported by Anderson and Wadsley [1]. Very recently, Yakubovich and Kireev [2] have refined the crystal structure of Na$_2$Ti$_3$O$_7$ reporting the space group (P2$_1$/m) and unit cell dimensions (a=9.133(2) Å, b=3.806(1) Å, c=8.556(2) Å, β=101.57(3)°). A total of about 130 phases of alkali titanates, including a dozen of sodium titanates are known [3]. The family of alkali titanates, represented by the general formula A$_2$Ti$_n$O$_{2n+1}$ (A= alkali metal and 2≤n≤9), is well known to have characteristic layered or tunnel type structures depending on n values. The layered members of this family have diverse potential applications as ion exchangers to intercalate organic guest molecules, to fix radioactive metal ions and to prepare several non alkali metal compounds in many cutting edge technologies [4]. Alkali titanates with unique layered structure may be used to

recover radioactive atoms from highly radioactive liquid wastes [5]. In Na$_2$Ti$_3$O$_7$, TiO$_6$ octahedra share edges at one level in a line group and each group is joined above and below to similar groups by further edge sharing, resulting in a zigzag ribbon structure [6]. It is also reported that Na$_2$Ti$_3$O$_7$, KTiNbO$_5$ and KNb$_3$O$_8$ have corner sharing octahedra only in one direction [7].

The intercalation of alkylammonium cations into layered titanate in the presence of macrocyclic compound has been studied by Ogawa et al. [8]. Recently, visible light induced electron transfer and long-lived charge separation in cyanine dye/layered titanate compounds have also been reported [9]. Moreover, Sauvet et al. [10] have reported synthesis and characterization of Na$_2$Ti$_3$O$_7$ and Na$_2$Ti$_6$O$_{13}$. Machida et al. [11] have investigated pillaring and photocatalytic properties of partially substituted layered titanates: Na$_2$Ti$_{3-X}$M$_X$O$_7$ and K$_2$Ti$_{4-X}$M$_X$O$_9$ (M=Mn, Fe, Co, Ni, Cu). The layered Na$_2$Ti$_3$O$_7$ powders of varying grain sizes have been prepared by solid state reaction of Na$_2$CO$_3$ and TiO$_2$ [12]. The structures of the titanates and the products, already undergone H$^+$ and Ag$^+$ exchange, have further been investigated by XRD, TEM and BET analysis and the influence of particle size and ion exchange

---

* Corresponding author. Tel.: +91 512 2315848; fax :+91 512 2315848.
*E-mail address:* shripalsharmappn@yahoo.co.in (Shripal).

property of the resulting products has been studied [12]. In a recent work, photochemical properties of $Cu^{2+}$ doped layered hydrogen titanates have been reported by Yanagisawa et al. [13]. The $Na_2Ti_3O_7$ is converted to $H_2Ti_3O_7$ by exchanging $Na^+$ with $H^+$ in HCl aqueous solution [14] and conversely $Na_2Ti_3O_7$ is recovered in the treatment of $H_2Ti_3O_7$ with NaOH solution [15]. Very recently, Zhang et al. [16,17] have reported the formation mechanisms of $H_2Ti_3O_7$ nanotubes. The electrochemical and calorimetric thermodynamical properties of $Na_2Ti_3O_7$ and $Na_2Ti_6O_{13}$ have also been determined by Holzinger et al. [18]

Kikkawa et al. [19] have investigated ceramic samples of $Na_2Ti_3O_7$, $K_2Ti_4O_9$ and their niobium-substituted products through a.c. conductivity measurements. $Na_2Ti_3O_7$, $K_2Ti_4O_9$, $K_{2-x}Rb_xTi_4O_9$ and their ($Na_2Ti_3O_7$ and $K_2Ti_4O_9$) iron and manganese doped derivatives have been investigated through electron paramagnetic resonance (EPR) and d.c. conductivity measurements by Shripal et al. [20–23]. Very recently, Shripal et al. [24] have further reported the dielectric-spectroscopic investigations on pure and manganese doped layered $Na_2Ti_3O_7$ ceramics.

Wang et al. [25] have proposed that larger $K^+$ should be able to replace $Na^+$ located between the layers of $Na_2Ti_2O_7$ compounds. However, no work has been reported in the literature on layered polycrystalline $Na_{2-x}K_xTi_3O_7$ (with X=0.2, 0.3, 0.4) ceramics. A schematic structural model for $Na_{2-x}K_xTi_3O_7$ is given in Fig. 1. Accordingly, it seems to be very interesting to synthesize and characterize $Na_{2-x}K_xTi_3O_7$ (with X=0.2, 0.3, 0.4) through dielectric-spectroscopic and a.c. conductivity investigations. The corresponding results are reported in this manuscript.
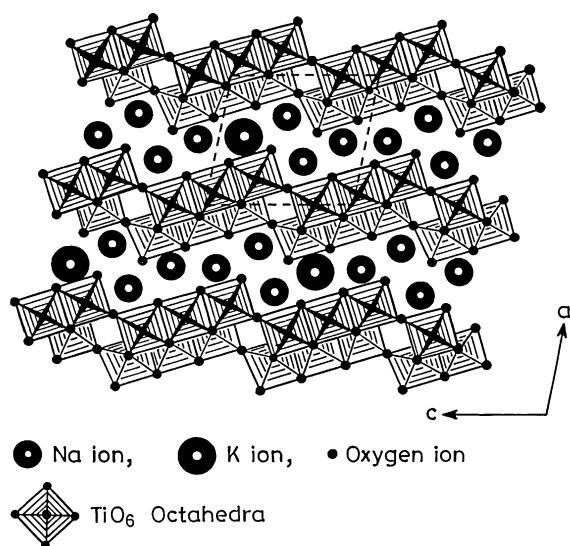


Fig. 1. Schematic structural model for $Na_{2-x}K_xTi_3O_7$ with the emphasis that potassium atoms are accommodated with sodium atoms in the widely opened interlayer space.

## 2. Experimental

Ceramic samples of $Na_{2-x}K_xTi_3O_7$ (X=0.2, 0.3, 0.4) were synthesized by taking $Na_2CO_3$ (Merck Germany, 99.9% pure), $K_2CO_3$ (Merck Germany, 99.9% pure), and $TiO_2$(Merck Germany, 99.9% pure) powders in stoichiometric molar ratio. After mixing under acetone, the powders were pre-heated at 1173 K for 16 h to drive off $CO_2$. The heated products were cooled to RT at the rate of 3 K per minute and reground to achieve fine powder. The pelletized samples, having 10 mm diameter and 1.5 mm thickness were obtained by applying isostatical pressure of 15 MPa on powder. These pellets were covered with the powder of the same composition to prevent reaction with the wall of the crucible and to diminish soda loss, and then, sintered at 1273 K for 16 h. These compositions of $Na_{2-x}K_xTi_3O_7$ for X=0.2, 0.3 and 0.4 are denoted as SPT-1, SPT-2 and SPT-3, respectively. XRD-patterns for all compositions were recorded by Richseifert Iso Debyflex 2002. Differactometer using $CuK\alpha$ radiation. The formation of these titanates (SPT-1, SPT-2 and SPT-3) is confirmed by the XRD-patterns obtained at room temperature (RT).

The sintered pellets were painted with a high purity silver paste and air dried. They were then mounted in the sample holder and evacuated up to $10^{-3}$ mbar for the electrical measurements. The loss tangent ($\tan\delta$) and parallel capacitance ($C_p$) of the pelletized samples were directly measured as a function of temperature and frequency by HP 4194A impedance analyzer. The relative permittivity ($\varepsilon_r$) and the bulk a.c. conductivity ($\sigma$) of the samples were calculated by using expressions:

$$\varepsilon_r = C_p/C_o \tag{1}$$

$$\text{Conductance } G = \omega C_p \tan\delta; \omega = 2\pi f \tag{2}$$

$$\text{and } \sigma = G(t/A) \tag{3}$$

where f is the frequency of a.c. signal, t is the thickness and A is the area of the cross-section of the pellet.

## 3. Results and discussion

The dependence of loss tangent ($\tan\delta$) on temperature in the range of 373–648 K at fixed frequencies for SPT-1, SPT-2 and SPT-3 are shown in Fig. 2 (a)–(c), respectively. It can be seen from these plots that the values of $\tan\delta$ remain invariant with the rise in temperature up to 473 K, while above 473 K, the usual increase in the values of $\tan\delta$ with the rise in temperature is observed with the indication of a broad relaxation type peak at around 600 K for all three compositions. The main difference is in numerical values showing that the average values of $\tan\delta$ decrease with the increase in potassium substitution, which is reflected well in $\tan\delta$ versus composition plots for 100 kHz at various
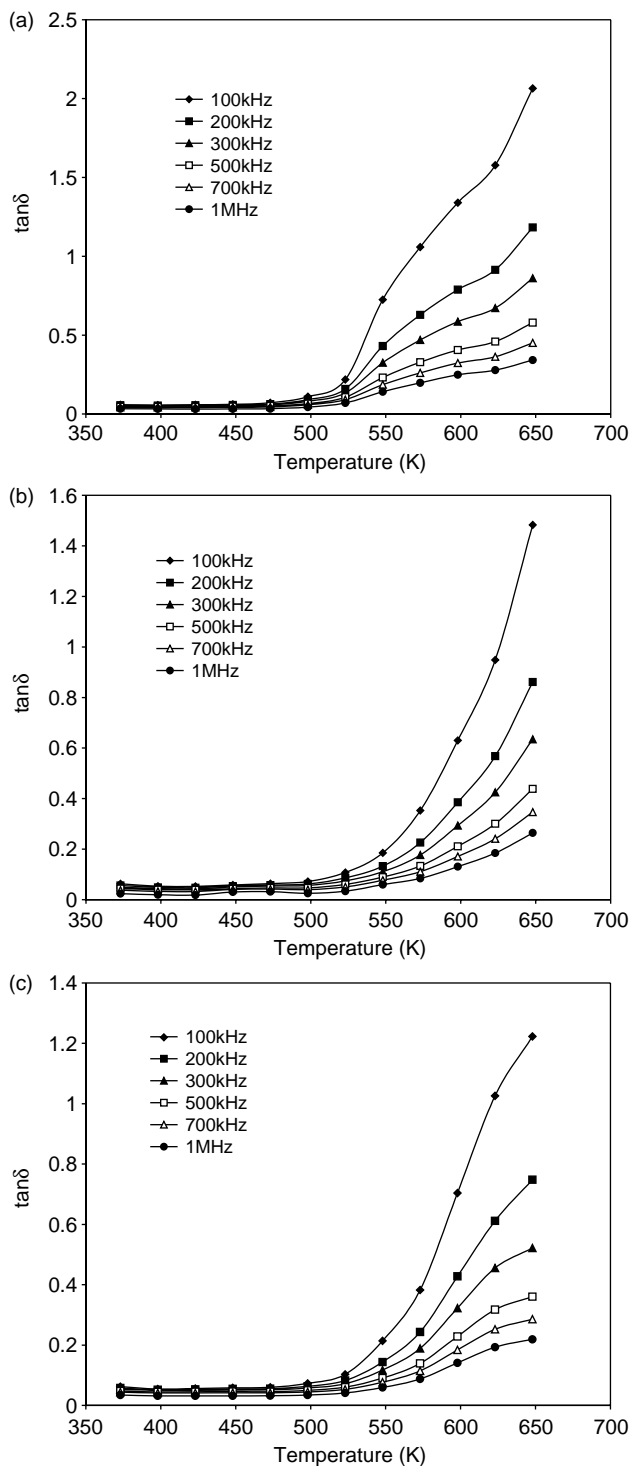
(a)



(b)



(c)



Fig. 2. Loss tangent (tanδ) versus temperature plots at different frequencies for (a) SPT-1, (b) SPT-2, (c) SPT-3



Fig. 3. Loss tangent (tanδ) versus composition plots of $Na_{2-x}K_xTi_3O_7$ for 100 kHz at different temperatures.

the number of ions that takes part in relaxation polarization continuously increases with the rise in temperature [27].

Fig. 4(a)–(c) show tanδ versus frequency curves in the temperature range of 373–648 K and frequency range of 100 kHz-1 MHz for SPT-1, SPT-2 and SPT-3, respectively. The results show that at lower temperatures tanδ decreases gradually when frequency increases but at higher temperatures, tanδ decreases exponentially with the rise in frequency. This may be an indication of losses due to the dipole mechanism [28] along with the motion of loosely bound ions, i.e. electric conduction [27].

Fig. 5(a)–(c) show the dependence of relative permittivity ($\varepsilon_r$) on temperature at fixed frequencies for SPT-1, SPT-2 and SPT-3, respectively. It can be seen that $\varepsilon_r$ remains almost invariant up to 473 K for all compositions. Above 473 K, however, $\varepsilon_r$ gradually increases with increasing temperature, forming small relaxation type of peak at 598, 448 and 623 K for SPT-1, SPT-2 and SPT-3, respectively. Above these temperatures, $\varepsilon_r$ increases rapidly with temperature showing maximum at 698 K. Thus, the trends of variations for all the compositions are similar except shifting of small relaxation type peak towards lower temperature (548 K) for SPT-2, which is again shifted towards higher temperature (623 K) for SPT-3. This may be an outcome of change in relaxation time due to increased potassium substitution in the interlayer space. Fig. 6 shows $\varepsilon_r$ versus composition plots for 100 kHz at various temperatures. The results reveal that the potassium substitution decreases $\varepsilon_r$ for SPT-2 and SPT-3 at all temperatures.

Since the tunnel and zig-zag layer structure titanates are composed of $TiO_6$ octahedra, which are so heavily distorted that the position of a central $Ti^{4+}$ ions deviates from the center of gravity of the surrounding six oxygen ions, dipole moment appears [29]. The zig-zag layer $Na_2Ti_3O_7$ has three dipole moments of 5.0, 5.8 and 6.2D +1D(debye)=

temperatures (Fig. 3). It should also be noted that the rapid increase in dielectric loss at higher temperatures for lower frequencies, is possibly arising due to space charge polarization [26]. The general increase of tanδ with temperature can be explained by assuming that

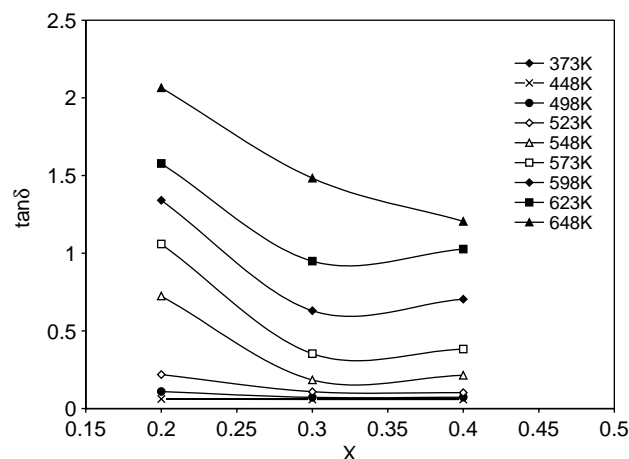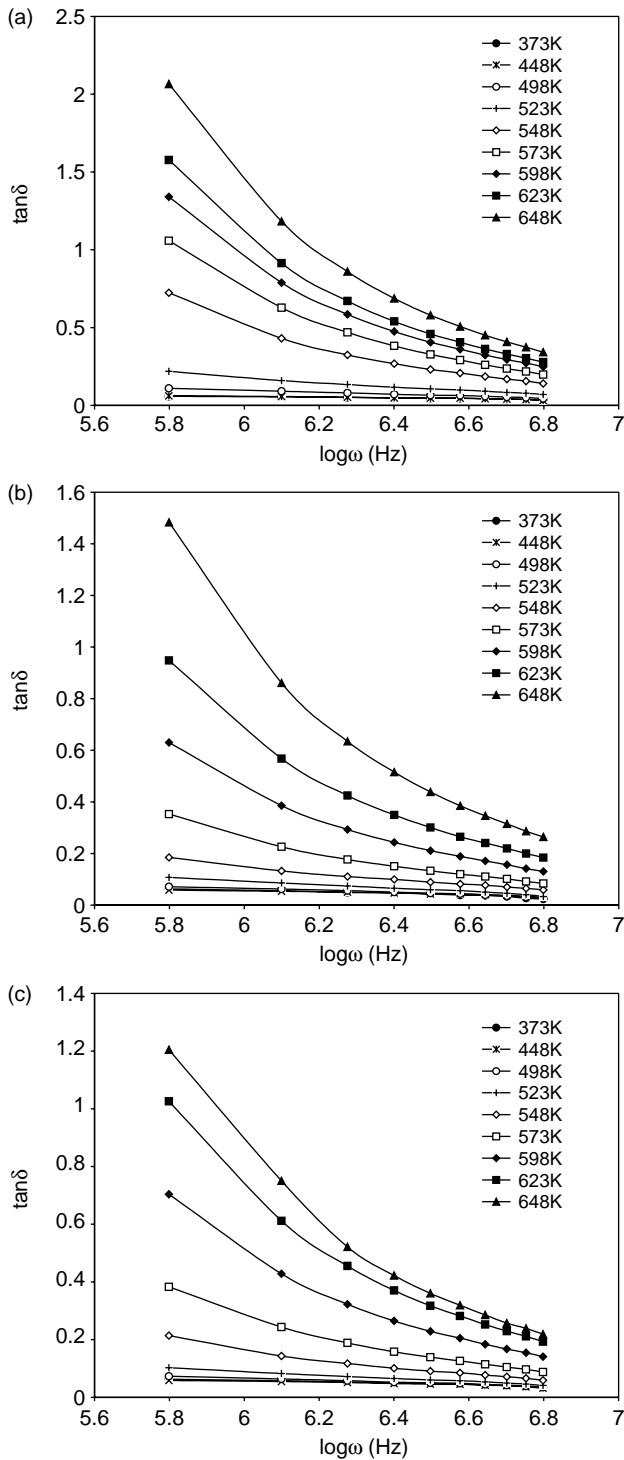Fig. 4. Loss tangent (tanδ) versus frequency plots at different temperatures for (a) SPT-1, (b) SPT-2, (c) SPT-3.

$3.33564 \times 10^{-30}$ cm [29]. Therefore, SPT-1, SPT-2 and SPT-3 will also have some dipoles moment. On exposure to the external field, the dipole experience a torque that tends to orient them in the field direction, thereby producing strong polarization effect and hence showing possible presence of spontaneous polarization. Also, $\varepsilon_r$ versus
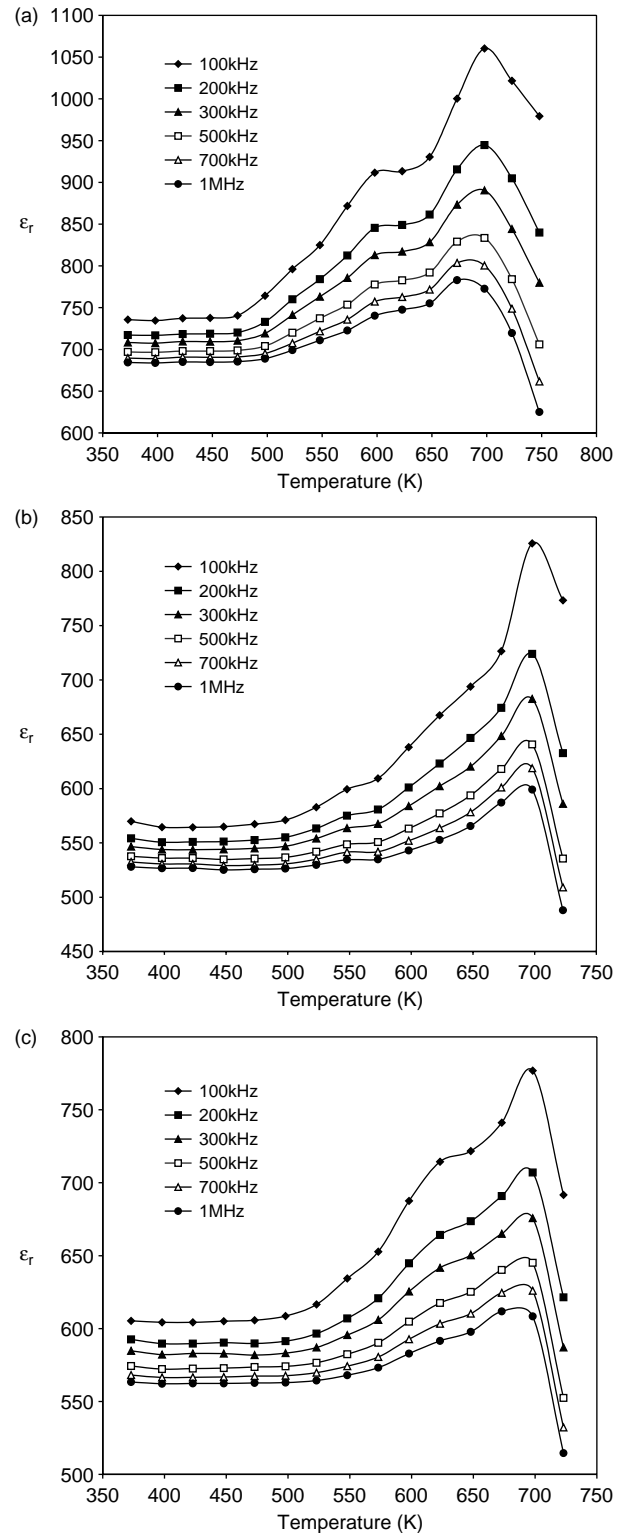


Fig. 5. Relative permittivity ($\varepsilon_r$) versus temperature plots at different frequencies for (a) SPT-1, (b) SPT-2, (c) SPT-3.

temperature curves have several maxima under applied a.c. field. Materials exhibiting the mechanism of spontaneous polarization dissipate much energy i.e., evolve heat [27], which is well reflected through tanδ versus
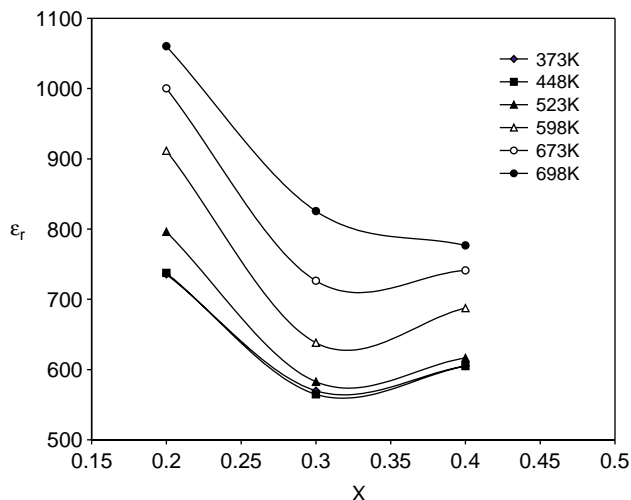
Fig. 6. Relative permittivity ($\varepsilon_r$) versus composition plots of $Na_{2-X}K_XTi_3O_7$ for 100 kHz at different temperatures.

temperature and frequency curves. Thus, pronounced peaks observed at 698 K for all compositions may be due to possible ferroelectric phase transition.

$\ln(\sigma T)$ versus 1000/T plots for SPT-1, SPT-2 and SPT-3 compositions are shown in Fig. 7(a)–(c), respectively. These plots can be divided into five regions.

**Region I (373–498 K):** In this region, trend of variations of a.c. conductivity is highly frequency dependent and almost temperature independent for all compositions. Various research groups [30–33] have been interpreting such results by proposing that a.c. conductivity due to electronic hopping conduction increases with the frequency ($\omega$) and is proportional to $\omega^s$, where $s$ is a parameter having value less than unity. Such frequency dependence has been attributed to a wide distribution of relaxation time due to spread in jump distances [34]. It is known that the zigzag layer titanate has the capability to efficiently separate photo excited holes and electrons in the manner of a tunnel structure titanate [29]. Thus, the mechanism of conduction in this region may be attributed to the electronic hopping conduction as proposed by Shripal et al. [21] for d.c. conductivity measurements.

**Region II (498–548 K):** In this region, for all compositions, a.c. conductivity is frequency and temperature dependent and possesses higher slope than region I. The results show that the slope of conductivity plots for SPT-2 and SPT-3 is lower than that for SPT-1 suggesting that the bigger $K^+$ ions are aggregated along with $Na^+$ ions in the interlayer space to take part in conduction. Therefore, as the potassium ions substitution further increases, the dilation of interlayer space occurs making conduction easy in this region for SPT-2 and SPT-3. It can be seen from the frequency dependence of
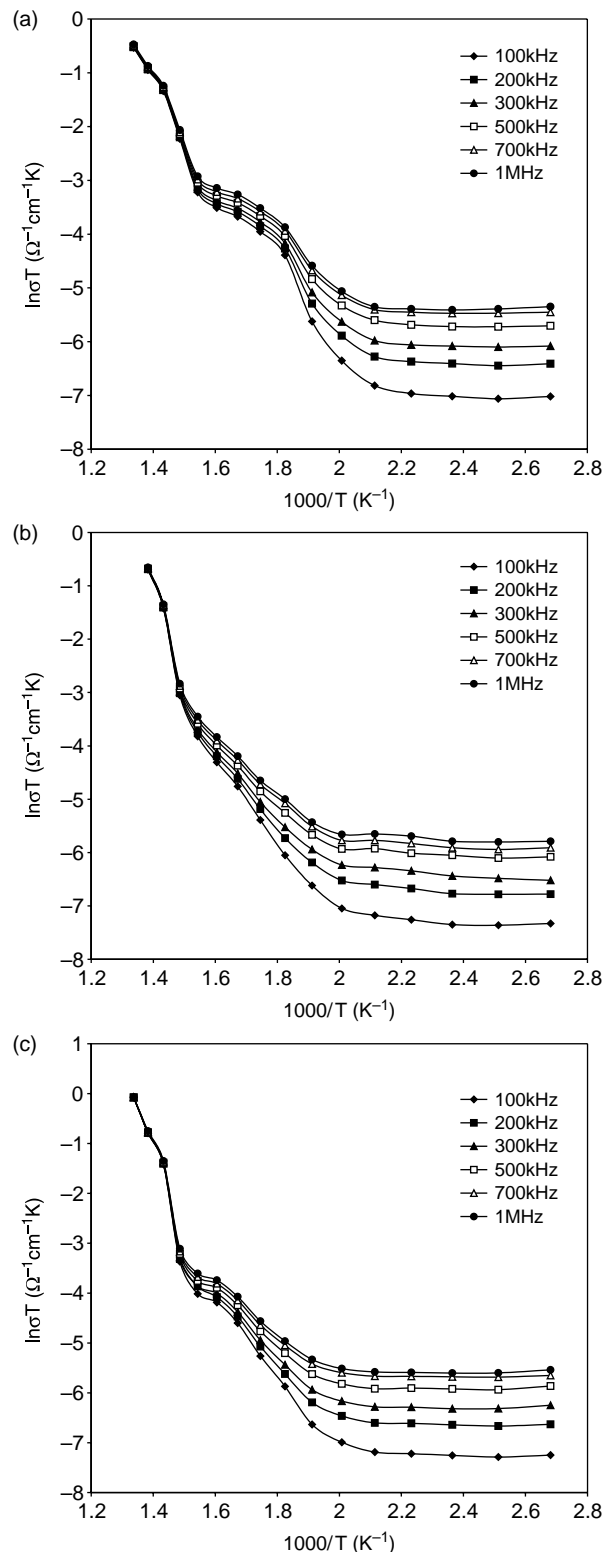


Fig. 7. $\ln(\sigma T)$ versus 1000/T plots at different frequencies (a) for SPT-1, (b) SPT-2, (c) SPT-3.

conductivity that hopping conduction also exists in this region.

**Region III (548–648 K):** In this region, the results show that the slope of conductivity plots for SPT-1 is
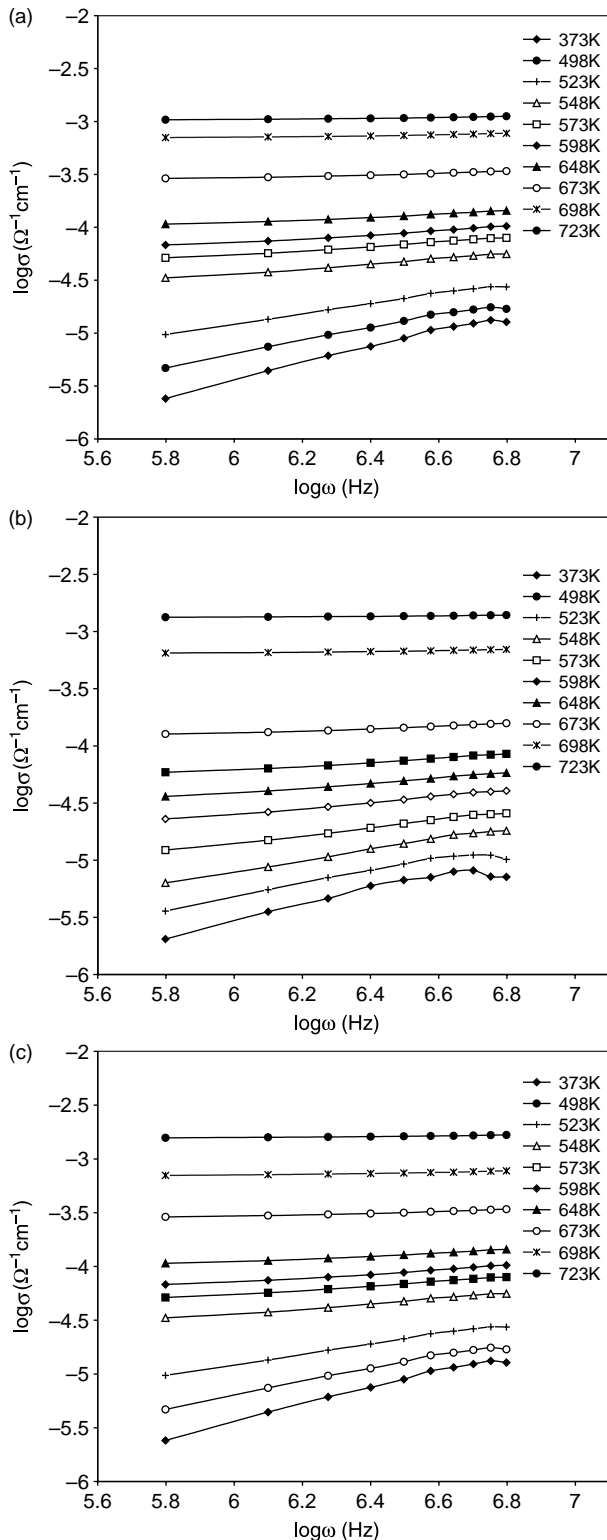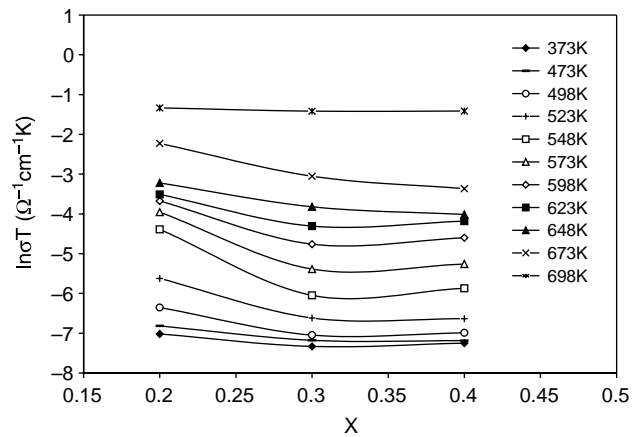
Fig. 9. $\ln(\sigma T)$ versus composition plots of $Na_{2-X}K_XTi_3O_7$ for 100 kHz at different temperatures.

of aggregation of $K^+$ and $Na^+$ ions in the interlayer space which then take part in conduction themselves together with other thermally induced charge carriers. The higher slope in the region for SPT-2 and SPT-3 may be an outcome of increased population of bigger $K^+$ ions taking part in conduction. It can be seen that small frequency dependence still persists indicating the presence of electronic hopping conduction as well.

**Region IV (648–698 K):** In this region, a.c. conductivity is highly temperature dependent but is almost frequency independent for all three samples. The higher conductivity may be attributed to the associated interlayer ionic conduction as reported earlier [21] with suppressed electronic hopping conduction.

**Region V (Above 698 K):** In this region, the nature of a.c. conductivity is temperature dependent and frequency independent. The trends of variations of a.c. conductivity for all compositions are similar and the slope is slightly lower than that found in region IV, which indicates that unassociated interlayer ionic conduction exists here as proposed by Shripal et al. [21].

Log($\sigma$) versus frequency plots for SPT-1, SPT-2 and SPT-3 are shown in Fig. 8(a)–(c), respectively. From these curves it can be seen that the dependence of conductivity on frequency decreases with the rise in temperature for all compositions. Thus, electronic hopping conduction is dominant at lower temperature only. Moreover, Fig. 9 shows the conductivity versus composition plots for 100 kHz at various temperatures. The results reveal a little change in the conductivity at lower temperatures (below 473 K). But the conductivity decreases appreciably for SPT-2 and then becomes almost constant for SPT-3 at higher temperatures. However, at 698 K, conductivity values are the same for all compositions, denying any role of the increased potassium substitution.



Fig. 8. Log($\sigma$) versus frequency plots at different temperatures for (a) SPT-1, (b) SPT-2, (c) SPT-3.

again lower than for SPT-2 and SPT-3. It can also be seen that frequency dependence of a.c. conduction still exists. The lower slope in this region as compared to the previous region for SPT-1 may be due to dissociation

## 4. Conclusions

The results of the present investigations may be summarized as:

 (i) For the first time layered polycrystalline $Na_{2-x}K_XTi_3O_7$ (with X=0.2, 0.3, 0.4) ceramics have been characterized through dielectric-spectroscopic and a.c. conductivity studies.
 (ii) Through dielectric-spectroscopic investigations the losses are attributed to the presence of dipoles along with the motion of loosely bound ions and space charge polarization at higher temperatures.
 (iii) The possible ferroelectric phase transitions at 698 K indicates ferroelectric behavior for all compositions.
 (iv) A.C. electrical conductivity studies show that the electronic hopping (polaron) conduction exists in a wide temperature range while dominance of inter-layer ionic conduction starts with the rise in temperature.
 (v) The dilation of zigzag interlayer space of $Na_2Ti_3O_7$ at the inclusion of potassium ions has been identified in this work. It has also been observed that the average value of loss tangent, relative permittivity and conductivity decreases with the increase in potassium substitution.
 (vi) Layered $Na_{2-X}K_XTi_3O_7$ (with X=0.2, 0.3, 0.4) ceramics can be put in the class of mixed ionic-electronic materials.

## Acknowledgements

## References

[1] S. Anderson, A.D. Wadsley, Acta Cryst. 14 (1961) 1245.
[2] O.V. Yakubovich, K.V. Kireev, Cryst. Rep. 48 (2003) 24.
[3] V.B. Nalbandyan, 6th European powder diffraction conference, Scientific programme and abstracts, Budapest, Hungary, Aug. 22–25, 1998, p. 233.
[4] S.-S. Lee, S.-H. Byeon, Bull. Korean Chem. Soc. 24 (2004) 1051.
[5] S. Kikkawa, M. Koizumi, in: S. Saito (Ed.), Fine Ceramics, Elsevier, U.S.A., 1988, p. 83–90.
[6] S. Anderson, A.D. Wadsley, Acta Cryst. 15 (1962) 194.
[7] C.N.R. Rao, B. Raveau, Transition Metal Oxides, VCH publishers, New York, 1995. p.103.
[8] M. Ogawa, Y. Takizawa, Chem. Mater. 11 (1999) 30.
[9] N. Miyamoto, K. Kuroda, M. Ogawa, J. Phys. Chem. B 108 (2004) 4268.
[10] A.L. Sauvet, S. Baliteau, C. Shopez, P. Fabry, J. Solid State Chem. 177 (2004) 4508.
[11] M. Machida, X.W. Ma, H. Taniguchi, J. Yabunaka, J. Kiyina, J. Mol. Cat. A Chem. 155 (2000) 131.
[12] J. Yang, D Li, X Wang, X Yang, L Lu, J. Mater. Sci. 38 (2003) 2907.
[13] M. Yanagisawa, S. Uchida, T. Sato, J. Inorg. Mater. 2 (2000) 339.
[14] A.D. Wadsley, W.G. Mumme, Acta Cryst. B 24 (1968) 392.
[15] H. Izawa, S. Kikkawa, M. Koizumi, J. Phys. Chem. 86 (1982) 5023.
[16] S. Zhang, L.-M. Peng, Q. Chen, G.H. Du, G. Dawson, W.Z. Zhou, Phys. Rev. Lett. 91 (2003) 256103.
[17] S. Zhang, Q. Chen, L.-M. Peng, Phys. Rev. B. 71 (2005) 014104.
[18] M. Holzinger, A. Benisek, W. Schnelle, E. Gmelin, J. Maier, W. Sitte, J. Chem. Thermodyn. 35 (2003) 1469.
[19] S. Kikkawa, F. Yasuda, M. Koizumi, Mater. Res. Bull. 20 (1985) 1221.
[20] Shripal, S.D. Pandey, Premchand, Solid State Commun. 69 (1989) 1203.
[21] Shripal, Premchand, S.D. Pandey, J. Mater. Sci.: Mater. Electron. 2 (1991) 89.
[22] Shripal, A.K. Misra, S.D. Pandey, R.P. Tandon, Eur. J. Solid State Inorg. Chem. 29 (1992) 229.
[23] ShripalR.P., Tandon, S.D. Pandey, J. Phys. Chem. Solids 52 (1991) 1101.
[24] Shripal, S. Badhwar, D. Maurya, J. Kumar, R.P. Tandon, in: K.K. Raina (Ed.), Advances in Condensed Matter Physics, Allied Publishers, New Delhi, 2005, p. 250.
[25] B.L. Wang, Q. Chen, R.H. Wang, L.-M. Peng, Chem. Phys. Lett. 376 (2003) 726.
[26] B.P. Das, R.N.P. Choudhary, P.K. Mahapatra, Mater. Sci. Eng. B. 104 (2003) 96.
[27] N.P. Bogoroditsky, V.V. Pasynkov, B. Tareev, Electrical Engineering Materials, Mir Publishers, Moscow, 1979 (Ch.1 and Ch.3).
[28] B. Tareev, Physics of Dielectric Materials, Mir Publishers, Moscow, 1979 (Ch.3).
[29] Ogura, S., Sato, K., Inoue, Y., Phys. Chem. Chem. Phys. 2 (2000) 2449.
[30] N.F. Mott, E.A. Davis, Electronic Processes in Non-crystalline Materials, Oxford Clarendon Press, 1971.
[31] G. Austin, N.F. Mott, Adv. Phys. 18 (1969) 41.
[32] M. Pollock, Philos. Mag. 23 (1971) 519.
[33] M. Bottger, V.V. Breyksin, Phys. Status Solidi B. 9 (1976) 79.
[34] M. Pollock, T.H. Geable, Phys. Rev. 122 (1961) 1742.